Biofilm thickness matters: Deterministic assembly of different functions and communities in nitrifying biofilms.

Carolina Suarez, [a,b]# Maria Piculell,[c] Oskar Modin,[b] Silke Langenheder[d] , Frank Persson,[b] Malte Hermansson[a]

[a]Department of Chemistry and Molecular Biology/Microbiology, University of Gothenburg, Sweden

[b]Water Environment Technology, Department of Architecture and Civil Engineering, Chalmers University of Technology, Sweden

[c]Veolia Water Technologies AB – AnoxKaldnes, Lund, Sweden

[d]Department of Ecology and Genetics/Limnology and Erken Laboratory, Uppsala University, Sweden

Running title: Biofilm thickness

#Address correspondence to Carolina Suarez, carolina.suarez@cmb.gu.se

Abstract word count: 229

Text work count: 4734

ABSTRACT

Microbial biofilms are important in natural ecosystems and in biotechnological applications. Biofilm architecture influences organisms' spatial positions, who their neighbors are, and redox gradients, which in turn determine functions. We ask if and how biofilm thickness influences community composition, architecture and functions. But biofilm thickness cannot easily be isolated from external environmental factors. We designed a metacommunity system in a wastewater treatment plant, where either 50 or 400 µm thick nitrifying biofilms were grown simultaneously on biofilm carriers in the same reactor. Model simulations showed that the 50 µm biofilms could be fully oxygenated whereas the 400 µm biofilms contained anaerobic zones. The 50 and 400 µm biofilms developed significantly different communities. due to deterministic factors were stronger than homogenizing dispersal forces in the reactor, despite the fact that biofilms experienced the same history and external conditions. Relative abundance of aerobic nitrifiers was higher in the 50 µm biofilms, while anaerobic ammonium oxidizers were more abundant in the 400 µm biofilms. However, turnover was larger than the nestedness component of between-group beta-diversity, i.e. the 50 µm biofilm was not just a subset of the thicker 400 µm biofilm with reduced taxa richness. Furthermore, the communities had different nitrogen transformation rates. The study shows that biofilm thickness has a strong impact on community composition and ecosystem function, which has implications for biotechnological applications, and for our general understanding of biofilms.

IMPORTANCE

Microorganisms colonize all surfaces in water and form biofilms. Diffusion limitations form steep gradients of energy and nutrient sources from the water phase into the deeper biofilm parts,

44 influencing community composition through the biofilm. Thickness of the biofilm will affect
45 diffusion gradients, and is therefore presumably important for biofilm composition. Since
46 environmental factors determine thickness, studies of how thickness influences biofilm functions
47 and community assembly, have been difficult to perform. We studied biofilms for wastewater
48 treatment with fixed thicknesses of 50 and 400 µm during otherwise similar conditions and
49 history. Despite growing in the same wastewater reactor, 16S rRNA gene sequencing and
50 confocal microscopy showed the formation of two different communities, performing different
51 ecosystem functions. Using statistical methods, we show for the first time, how biofilm thickness
52 influences community assembly. The results help our understanding of the ecology of microbial
53 biofilms, and in designing engineered systems based on ecological principles.

INTRODUCTION

Biofilms are dense communities, encased in a polymer matrix, attached to a surface and/or each other (1) with a high microbial diversity compared to the bulk water system (1-3). Microbial biofilms are important in aquatic ecosystems and are useful in many biotechnological applications, such as wastewater- or drinking water treatment. In nitrogen removal from wastewater, moving bed biofilm reactors (MBBRs) are used at many wastewater treatment plants (WWTPs). Here biofilms grow on so-called carriers, which move freely in the bioreactor (Fig. 1C). An MBBR can be seen as a metacommunity (4), just as other WWTP systems such as activated sludge flocs and granules, where each free-floating biofilm carrier represents a local community. The local communities have defined boundaries and are separate, but linked by dispersal with all other biofilm carriers in the reactor, in this case fed with wastewater from a full-scale WWTP to form nitrifying biofilms. The reactor represents the regional level and is assumed to be a spatially implicit system, i.e. dispersal is likely to be equal between all carriers (4).

The mechanisms of community assembly are central in microbial ecology and in our understanding of formation of biodiversity in all ecosystems (5, 6), including microbial communities in biofilms (7). Communities are formed by deterministic and stochastic factors that include four major ecological processes: selection, drift, dispersal and speciation (8). Selection, i.e. the sorting of species by prevailing local abiotic and biotic conditions, is deterministic, while drift results from stochastic birth and death events (6, 8). If local communities are further exposed to stochastic dispersal from the regional species pool (as we can assume to be the case of bioreactors in WWTPs), the expected result is that the abundance of a

77 taxon in a local community can be predicted based on its respective abundance in the regional
78 species pool and thereby follows neutral distribution patterns (9, 10). However, dispersal can
79 also be deterministic if microorganisms differ in their ability to disperse within the complex
80 spatial biofilm matrix or if their propagation is affected by interactions with species already
81 present in the biofilm.

82

83 Selection has been suggested as the major mechanism for community assembly in stream
84 biofilms (11-13), and other biofilms (14), while for biofilms within lakes linked by dispersal,
85 both stochastic and deterministic factors were shown to be important (15). The importance of
86 both stochastic and deterministic factors was shown in an elegant study using parallel microbial
87 electrolysis cells incubated with wastewater (16). Other studies in wastewater activated sludge
88 systems have shown the importance of deterministic and stochastic factors (17-20).

89

90 Deterministic assembly in biofilms could be due to specific mechanisms: Firstly, diffusion
91 limitations form steep gradients of electron donors and acceptors in biofilms, which result in
92 structured micro-environments. Examples are found in biofilms in WWTPs used for nitrification
93 (i.e. oxidation of ammonium to nitrate) during the nitrogen removal process (21, 22). Here
94 population stratification typically occurs; ammonia oxidizing bacteria (AOB) are found closest to
95 the oxygenated water and nitrite oxidizing bacteria (NOB) below the AOB (23-26). If oxygen is
96 consumed, anaerobic ammonium oxidizing (anammox) bacteria can establish in the deeper parts
97 of the biofilm (23, 27, 28). Similarly, in other multispecies biofilms anaerobic sulfate reducing
98 bacteria are found in the biofilm interior (29). However, functions in microbial communities are

not always sorted according to such a thermodynamic "redox tower" of electron acceptor (30). This makes detailed *a priori* predictions of community structure in biofilms difficult. Secondly, in addition to gradients, it was realized early on that microbial biofilms are in fact complex structures and not homogenous layers of randomly distributed organisms (3) and, ever since, architecture has been viewed as an important biofilm property. The intricate biofilm architecture consists of towers, mushroom-like structures and water filled channels (1, 2, 7, 31). If biofilms differ in their architecture, dispersal effects could influence community assembly by changing the colonization surface available. Furthermore, microorganism with deterministic dispersal might show preference towards different types of biofilms.

Thickness will influence biofilm architecture and redox gradients and thus generally the local biofilm environment. However, the experimental evidence for effects of thickness on architecture, community structure and function has been difficult to obtain because biofilm thickness is the result of environmental conditions such as flow (1, 7, 32-34), nutrient conditions (24), development age of the biofilm (34), carbon to nitrogen (C/N) ratios (25) and temperature (35). In most experimental systems, thickness cannot easily be isolated from these environmental factors that themselves can influence the community structure and functions.

Recently, a biofilm carrier with a defined grid wall height that defines the biofilm thickness was designed (Z-carriers, Veolia Water Technologies AB – AnoxKaldnes, Lund, Sweden) (36-38). These carriers allow stringent experiments with different biofilm thicknesses, which have shown that thickness can affect some biofilm functions (38, 39), evenness (39), biofilm architecture

(37), abundance of key organisms (37, 39) and functional stability after a disturbance (37). Beside the opportunities to gain basic ecological knowledge by designing new experiments, the ability to control biofilm thickness opens for new process configurations in WWTPs. In this study, a pilot nitrifying bioreactor was filled with a mixture of Z-carriers with biofilm thicknesses of 50 and 400 µm. Thus, environmental conditions and history of the biofilms were the same. We ask if thickness, in itself or via diffusion effects or other mechanisms, is important for bacterial community structure, and if so, what the possible mechanisms of community assembly would be. The thicknesses we investigated are within the range commonly found in natural- as well as in man-made biofilms (25, 26, 32, 40, 41).

Differences in communities, i.e. beta-diversity between thin and thick biofilms, could arise due to (a) turnover (species replacement) or (b) nestedness resulting from differences in alpha-diversity (42), which can both result from deterministic (e.g. environmental gradients) and stochastic factors (e.g. dispersal and drift) (42, 43). For example, as thicker biofilms have larger volume and surface-area, they are by chance expected to be colonized by more species, leading to higher richness. A possible deterministic mechanism for higher richness in 400 compared to 50 µm biofilms would be if redox profiles differ between them. Generally, the nitrifying bioreactor is an oxic environment and the presence of aerobic taxa is expected. However, if anoxic regions exist in thick biofilms, this would allow the establishment of anaerobic taxa, increasing species richness. In this case, we hypothesize that the 50 µm biofilm community would be a subset of the richer 400 µm biofilm community, due to anaerobic taxa being restricted to the thicker 400 µm biofilms, while the same aerobic taxa occur in both the 50 and 400 µm biofilms. Alternatively, turnover, i.e. differences in species identity, could arise if

144 biofilms of different thickness have different environmental conditions apart from redox profiles.
145 Finally, we also measured rates of nitrogen transformations in the two biofilms and investigated
146 whether possible differences in ammonia- and nitrite removal rates between biofilms of distinct
147 thicknesses are primarily linked to differences in taxa richness (i.e. nestedness) or identity (i.e.
148 turnover) and discuss the implications of the results for wastewater treatment.

149

150 **RESULTS**

151 **Two different biofilms**

152 We grew biofilm communities with a maximum thickness of 50 μm and 400 μm together in the
153 same bioreactor; these communities are referred to as Z50 and Z400. CLSM images of EPS
154 stained biofilm cryosections confirmed that carrier design limited biofilm thickness (Fig. 1A and
155 B).

156

157 **Alpha and beta diversity**

158 The alpha diversity parameters richness (^0D), first-order diversity (^1D) and evenness ($^1D/^0D$)
159 (Fig. 2A), were all significantly higher for the thick Z400 biofilms than for the thinner Z50
160 biofilms (Welch t-test, $p<0.05$). We also estimated beta diversity using the presence-absence
161 based Sørensen index (β_{sor}), which showed that Z50 and Z400 communities were different
162 (PERMANOVA β_{sor}, $p=0.002$, $r^2=0.50$) (Fig. 2B).

163

We used null modelling to estimate the standardized effect size (SES) for β_{sor}. We observed that β_{sor} values for between-group comparisons, i.e. between Z50 and Z400, were higher than expected by chance β_{sor} values for between-group comparisons ($SES_{\beta sor} > +2$) (Fig. 3A) indicating that between-group differences were likely deterministic. On the contrary, observed β_{sor} values for within-group comparisons, i.e. between the carriers of the same type, were not more different than expected by chance ($|SES_{\beta sor}| < 2$) (Fig. 3A). In addition, estimation of the quantitative RC_{BRAY} metric, also indicated that Z50 and Z400 communities were in average more dissimilar than the null expectation (between-group $RC_{BRAY} > +0.95$)

To determine whether the between-group beta diversity was due to nestedness or turnover, we estimated the components of β_{sor}; turnover (β_{sim}) and dissimilarity due to nestedness (β_{sne}) using the Baselga framework (42) (Fig. 3B), to estimate the β_{ratio} (44). When β_{ratio} is smaller than 0.5, beta diversity is dominated by turnover rather than β_{sne} (44). We observed a between-group β_{ratio} lower than 0.5 (Fig. 3C). The differences between the Z50 and Z400 communities due to turnover were significant (PERMANOVA β_{sim}, $p=0.001$, $r^2=0.34$). Thus, the beta diversity between the Z50 and Z400 communities was caused by both nestedness and turnover, with turnover being more important.

Differences in relative abundance of taxa between Z50 and Z400 were estimated using DESeq2. We found differential abundance ($p_{(adj)}<0.01$, DESeq2) for 45% of the sequence variants (SVs) analyzed with DESeq, while for the top 40 most abundant SVs, 32 had different abundance between Z50 and Z400 (Fig. S1). Among the fraction with differential abundance, 26% of SVs

were more abundant in Z50, and 74% were more abundant in Z400. The effect of thickness on relative abundance, if any, differed among taxa (for example see Fig. S1).

Between-group sorting of nitrifiers and anammox bacteria

The relative read abundance of the nitrifiers, *Nitrosomonas*, *Nitrospira* and *Nitrotoga*, was lower in the Z400 biofilms with *Nitrotoga* being almost restricted to Z50 (Fig. 4A). The same trends were noticed using quantitative fluorescence in situ hybridization (qFISH; Fig. 4C; Welch's t-test, $p<0.05$). It was not possible to detect by qPCR if comammox were present due to non-specific amplification using *Nitrospira amoA* primers (45).

Interestingly, we observed the anammox bacterium *Brocadia* in the Z400 biofilms, but it was almost absent in the Z50 biofilms (Fig. 4A). This was supported by qFISH (Welch t-test $p<0.001$) (Fig. 4C). Sorting of bacteria between thick and thin biofilms was not only limited to primary producers (i.e. autotrophic nitrogen converters) but also seen among the predatory *Bdellovibrionales*. *Bacteriovorax* had a higher abundance in the Z50 communities, while some SVs classified as *Bdellovibrio* were more abundant in either Z400 or Z50 (Fig. S2).

FISH analyses of biofilm cryosections showed that the Z400 biofilm was stratified, e.g. with *Nitrospira* being more abundant in the middle of the biofilm and the anaerobic anammox bacteria being present in the deeper layers; a lack of stratification was observed *Nitrosomonas* (Fig. 5A and 5B). In the thin Z50 biofilms, no stratification was observed as the AOB and NOB

207 populations were located side by side (Fig. 5C). The calculated dissolved oxygen (DO)
208 concentration profiles in the biofilms are shown in Fig. 6; the results give a range of possible DO
209 concentration profiles, which are shown as shaded regions. The model predicts that Z50 biofilms
210 can be fully oxygenated but may also have anoxic regions, whereas the Z400 biofilms contain a
211 completely anoxic region in its deeper parts in all tested scenarios.

212

213 **Nitrogen transformation rates**

214 Two types of tests were performed separately on the Z50 and Z400 carriers; (i) actual activities
215 tested in a continuous laboratory trial, with the same incoming water as in the 0.5 m^3 reactor and
216 (ii) potential activities tested in batch trials where excess nitrogen was added. For all trials,
217 removal rates are reported per surface area and day. Actual rates of net NO_3^- production were
218 1.4-1.5 gNO_3^--N/m^2, d for Z50 and 0.68-0.72 gNO_3^--/m^2, d for Z400. To estimate NO_3^-
219 production per nitrifier abundance, it is necessary to consider differences in biomass between
220 carriers. We estimate that the total nitrifier biomass per carrier surface was about the same in
221 Z50 and Z400 (Fig. 4B). Therefore, per nitrifier biomass, net NO_3^- production was higher in Z50
222 than in Z400.

223

224 In the aerobic potential tests for net NH_4^+ removal (Fig. 7A), net NO_3^- and net NO_2^-production
225 (per carrier area) was higher for Z50 than Z400 biofilms (ANCOVA, $p<0.05$), while the rate of
226 net NH_4^+ removal was not significantly different between Z50 and Z400 (ANCOVA, $p>0.05$).
227 The aerobic potential removal of NO_2^- (Fig. 7B) was significantly higher for Z400 than for Z50
228 (ANCOVA, $p<0.05$). Finally, in the anoxic potential trials, in which NH_4^+ and NO_2^- were added

229 simultaneously (Fig. 7C), removal of NO_2^- was significantly higher for Z400 than for Z50
230 (ANCOVA, $p<0.05$), while no significant removal or production of NH_4^+ was seen for either
231 Z50 or Z400.

232

233 **DISCUSSION**

234 Although incubated in the same bioreactor and experiencing the same conditions and the same
235 history, different microbial communities developed on carriers with thin and thick biofilms (Fig.
236 2B). The thicker Z400 biofilm had a higher richness and evenness than the thinner Z50 biofilm
237 (Fig. 2A) and our results are therefore in agreement with known positive species-area
238 relationships for microbial communities (46). Moreover, similar to our results, Torresi et al. (39),
239 focusing on micro-pollutant degradation, also found a significant higher evenness in thicker
240 biofilms.

241

242 A null model approach was used to investigate if the differences in beta-diversity between Z50
243 and Z400 were due to deterministic or stochastic factors while accounting for the large
244 differences in richness between Z50 and Z400 (47). The results showed that the between-group
245 beta-diversity was higher than expected by chance (Fig. 3A), suggesting deterministic assembly
246 due to differences in biofilm thickness. This result was also confirmed by the fact that biofilm
247 thickness significantly affected the relative abundance of the majority of the most abundant
248 individual taxa, meaning that they showed clear preference for either thin or thick biofilms (Fig.
249 S1). Some turnover among the Z50 and Z400 replicates was observed, and was also expected
250 due to ecological drift. Low SES values (Fig. 3A) suggest stochastic assembly among replicates,

however, the relative importance of drift and dispersal cannot be disentangled with the experimental setup used here. In addition, due to the limited number of within-group replicates, these results should be interpreted with caution. Because MBBRs allow a high level of replication in communities linked by dispersal, a similar setup to the one use here with higher replication could be used to study stochastic assembly and to confirm the possible existence of alternate states (16, 48). Overall, other studies have shown that stochastic and deterministic processes can co-occur in biofilms (15, 17, 18). Our results suggest that the importance of deterministic vs. stochastic assembly depends on biofilm thickness: assembly would be deterministic between biofilms of different thickness, while assembly would likely be stochastic among biofilms with the same thickness.

Our hypothesis was that the communities in Z50 would be an aerobic subset of the ones in Z400. Thus, beta-diversity between Z50 and Z400 would largely be due to nestedness, whereas turnover would have a small contribution. This was expected due to different redox profiles between Z50 and Z400 biofilms (Fig. 6) which could create nestedness; oxygen in the thin Z50 biofilm inhibit the growth of obligate anaerobes like anammox bacteria (49). Thus, richness in Z400 would be higher, because the community is a mixture of aerobic and anaerobic taxa. Surprisingly, although between-group β_{sne} was observed, the β_{ratio} was below 0.5 (Fig. 3C), indicating that beta-diversity was dominated by turnover. Thus, the Z50 biofilm was not just a subset of the oxic upper layers of the Z400 biofilm, but differences were primarily due to turnover of taxa. For example, *Nitrotoga* was observed in Z50, but was nearly absent in Z400 (Fig, 4, S1), which cannot be easily explained by redox profiles. Independently of the

mechanism, it appears that thin biofilms favor the NOB *Nitrotoga*, which could have consequences for operational strategies in wastewater treatment.

Redox profiles (Fig. 6) explain the stratification of some taxa like anammox bacteria and *Nitrospira* in the Z400 biofilm (Fig. 5B). *Nitrosomonas* was the dominant population at the top of the Z400 biofilm (Fig. 5A, S3C) and was also abundant in Z50. However, *Nitrosomonas* aggregates were present throughout the Z400 biofilm, even in regions predicted to be anoxic (Fig. 5A, 5B). Furthermore, in the thin Z50 biofilm, *Nitrospira* was seen alongside *Nitrosomonas* (Fig. 5C), and here its relative abundance was actually higher than in Z400. Hence redox profiles alone cannot explain the distribution of taxa in the reactor. The fact that redox is not the only determinant of the distribution of microorganisms, even in strongly structured environments like sediments, has been noted (30). The Z50 and Z400 biofilms also differed in their spatial structure, with Z50 being more dense and having a smoother architecture, compared with the Z400 (Fig. 1) (37); furthermore extracellular nucleic acids were observed in Z400 but not in Z50 (data not shown). Thus, these differences could contribute to the deterministic turnover observed in this study, by either selection or deterministic dispersal. Another possible mechanism for between-group species turnover are biotic interactions. For instance, some SVs within the predatory *Bdellovibrionales* were differently distributed between the biofilms (Fig. S2). It is plausible that the two biofilms represented different prey communities that in turn shaped the predatory *Bdellovibrionales* communities. Such influence on the predatory *Bacteriovorax* has been shown, even for closely related preys (50, 51). Furthermore, Torsvik et al. suggested that predation can act as a major factor driving prokaryotic diversity (52). Hence, biological

295 interactions, such as predation, could have had a large effect on these biofilm communities, as
296 shown for other wastewater biofilms (53).

297

298 Differences in community composition between Z50 and Z400 were to a larger extent
299 determined by turnover than nestedness. Therefore, we predict that differences in nitrogen
300 transformation rates among them might not necessarily be linked to the differences in richness
301 and evenness between Z50 and Z400. This is despite previous examples that have shown that
302 species richness (46) and evenness (54) may by themselves lead to higher productivity. Similar
303 to earlier studies (39), we found that the thinner biofilm had higher net NO_3^--production rates,
304 despite having lower richness. This supports that species composition might be more important
305 than alpha-diversity for some processes (55), such as nitrification. Moreover, increased evenness
306 in the Z400 compared to Z50 biofilms could have resulted in lower abundance of specialized
307 taxa (56, 57), such as *Nitrosomonas* and *Nitrospira*, and thereby decrease net NO_3^--production
308 rates. Despite differences in relative abundance in *Nitrosomonas*, their absolute abundance was
309 estimated to be the same in both Z50 and Z400. When measuring *Nitrosomonas* abundance, it is
310 assumed that the entire population might contribute to aerobic ammonia oxidation. However we
311 observed *Nitrosomonas* microcolonies throughout the Z400 biofilm depth (Fig 5A); the ones
312 living in the deeper parts of the biofilm might have little or no access to oxygen (58). These
313 *Nitrosomonas* cells could have low nitrification activity or they could represent strains capable of
314 anaerobic respiration (59). Therefore, *Nitrosomonas* abundance might not be directly correlated
315 with nitrification rates in thick biofilms.

316

317 A different ecosystem function, anaerobic NO_2^- removal could occur via denitrification,
318 anammox or DNRA. We observed higher anaerobic NO_2^- removal rates in Z400 than Z50. This
319 could be due to deterministic assembly, where the presence of anaerobic regions in Z400, likely
320 allowed the establishment of taxa that could use NO_2^- as electron acceptor. This agrees with a
321 previous study (39), showing that an increase in biofilm thickness could lead to the emergence of
322 new functions. Higher aerobic NO_2^- removal in Z400 could occur because of NO_2^- being used
323 both as electron donor by NOB, and as electron acceptor by anaerobic taxa in anaerobic regions
324 of the Z400.

325

326 In summary, we show that biofilm thickness can influence bacterial biofilm community
327 composition despite the fact that history and all other external conditions are similar. The
328 differences in communities between thin and thick biofilms were likely deterministic, but
329 differences could not always be easily explained just by differences in redox conditions (*cf*. (30).
330 Between-group beta-diversity was due to both nestedness and turnover, but dominated by
331 turnover. Furthermore, based on potential and actual measurements, the two communities
332 performed ecosystem functions at different rates, which support the idea that beta-diversity in the
333 same metacommunity can lead to the emergence of multiple ecosystem functions (60). Results
334 from these and similar experiments can be used in design of new process strategies in wastewater
335 treatment. For example, thinner nitrifying biofilms could be combined with ticker biofilms to
336 increase the number of ecological functions (39). Finally, bioreactors are well suited for
337 experiments that can help disentangle factors of community assembly, as also suggested before
338 (6).

339

MATERIALS AND METHODS

The reactor

The 0.5 m^3 MBBR was located at the Sjölunda WWTP in Malmö, Sweden. The reactor was fed with effluent from a high-rate activated sludge process treating municipal wastewater (a feed with low carbon to nitrogen ratio). The average reactor load during one month before the sampling was 0.48 kg NH_4^+-N/m^3,day and the NH_4^+ removal was 42%, at a pH of 7.4; dissolved oxygen (DO) concentration of 5 mg/L; and temperature of 17°C. After 261 days of operation, carriers were sampled for DNA-sequencing, FISH and activity tests to determine nitrogen transformations. The reactor contained a mixture of Z50 and Z400 carriers (Veolia Water Technologies AB – AnoxKaldnes, Lund, Sweden) at a total filling degree of approximately 30%. Thickness of the biofilm in Z-carriers is limited by a pre-defined grid wall height (36). Samples for optical coherence tomography measurements were taken on day 272 and data showed a biofilm thickness of 45 ±17 and 379 ± 47 (mean ± S.D.) µm for Z50 and Z400, respectively (37).

Nitrogen transformation activity tests

Actual activity was measured in 1 L reactors in duplicate: Two reactors with 100 Z50 carriers each, and two with 100 Z400 carriers each. The incoming water was the same as the water feeding the 0.5 m^3 reactor. At the time of measurement, the NH_4^+-N concentration was 19.6 mg/L, the DO was 5.5 mg/L, and the temperature was kept at 20°C. Mixing was achieved by supplying a gas mix consisting of N_2-gas and air to the bottom of the reactors at an approximate total flow of 3 L/min and the DO was controlled to 5.5 mg/L by adjusting the amount of air in

361 the gas mix. Nitrification rates were measured from mass balance as NO_2^--N and NO_3^--N
362 mg/m^2,day.

363

364 For the potential activity trials 3 L reactors, containing 400 carriers each, were used. The
365 substrate consisted of $NaHCO_3^-$ buffer, pH adjusted to 7.5 using H_2SO_4, with phosphorous and
366 trace minerals added in excess (36). Aerobic removal of NH_4^+ (starting concentration 35.2 NH_4^+-
367 N mg/l) and NO_2^- (starting concentration 32.5 NO_2^--N mg/l) were measured separately in two
368 different trials at 20˚C for 1 hour, with sampling every 10 minutes. Mixing was achieved by
369 supplying a gas mix consisting of N_2-gas and air to the bottom of the reactors at an approximate
370 total flow of 3 L/min. DO was controlled to 5.5 mg/L by adjusting the amount of air in the gas
371 mix. Anaerobic trials of simultaneous removal of NH_4^+ and NO_2^- (starting concentrations 35.5
372 NH_4^+-N and 36.1 NO_2^--N mg/l) was measured at 30˚C and were run for 2 hours with sampling
373 every 20 minutes. Mixing was achieved by N_2-gas from the reactor bottom. Before commencing
374 the trials, the reactor with substrate was fed with N_2-gas until the DO concentration was
375 negligible and thereafter the carriers were added and the trials begun. Water samples were
376 collected and filtered through 1.6 µm Munktell MG/A glass fiber filters and analyzed for NH_4-N,
377 NO_2-N and NO_3-N using standard Hach-Lange kits (LCK 303, 342 and 339, respectively).

378

379 **Fluorescence in situ hybridization (FISH)**

380 FISH on cryosections and qFISH were done as previously described (37). The FISH probes used
381 in this study are shown in Table S1. EPS and total nucleic acids on biofilm cryosections were

382 stained with the FilmTracer SYPRO Ruby biofilm matrix stain and SYTO 40 (Thermo Fischer
383 Scientific, USA), respectively. See Text S1, for details.

384

385 **Simulation of dissolved oxygen (DO) concentration profiles**

386 A mathematical model was developed for simulating DO concentration profiles in the biofilms.
387 The model considered the activities of aerobic heterotrophic bacteria, AOB and NOB. The bulk
388 liquid concentrations of substrates (DO, nitrite, ammonium, and organic compounds), the
389 measured biofilm densities, the microbial community compositions (as determined by FISH), the
390 distribution of different functional groups of microorganisms in the biofilm (as measured by
391 FISH), and kinetic coefficients from the scientific literature were used as input parameters. The
392 thickness of the liquid boundary layer that limits diffusion of soluble substrates, including DO,
393 from the bulk liquid to the biofilm was determined by comparing the ammonium oxidation rates
394 calculated by the model to those measured during the nitrogen transformation activity tests.
395 Since the exact concentrations of active biomass in the biofilms were unknown, the model was
396 solved for different scenarios in which the active biomass was assumed to make up 20-80% of
397 the measured total dry solids. It should be noted that the model only considers biofilm
398 heterogeneity in one dimension (the depth direction). Layers parallel to the substratum are
399 assumed to be homogenous. Real biofilms are three-dimensional structures containing channels
400 and voids, which may allow oxygen transport into deeper regions locally. See Text S1 for details.

401

402 **DNA extraction and 16S rRNA gene sequencing**

DNA was separately extracted from ten Z50 and ten Z400 carriers. DNA extraction, PCR and high throughput amplicon sequencing of 16S rRNA gene was done as previously described (61) with some modifications. Sequence variants (SVs) were generated for finer resolution of taxa (62, 63). See Text S1for details. Raw sequence reads were deposited at the NCBI Sequence Read Archive, no. SRP103666.

Statistics

Data was analyzed in R (R Core Team 2018), using the packages Phyloseq (64), Vegan (65), DESeq2 (66) and betapart (42). Differential abundance of SVs was estimated with DESeq2 (66, 67), without random subsampling before the analysis. After independent filtering in DESeq2, 2578 of 3690 SVs were analyzed. A $p_{(adj)} < 0.01$ value (DESeq2) was used as criterion for statistical significance. Subsampling to even depth was done prior to estimation of alpha-diversity and beta-diversity. Alpha-diversity was calculated as the first two Hill numbers (68), ${}^{0}D$ (richness) and ${}^{1}D$ (exponential of Shannon-Wiener index). Evenness was estimated as $({}^{1}D/{}^{0}D)$. Beta-diversity was estimated as pairwise Sørensen (β_{sor}) dissimilarities, a presence-absence metric. Principal coordinate analysis (PCoA) was used for ordination. Permutational multivariate analysis of variance (PERMANOVA) (69) was used test for significant difference between group centroids. The components of β_{sor}, turnover (β_{sim}) and dissimilarity due to nestedness (β_{sne}), were estimated as described by Baselga et al. (42) and used to calculate the beta diversity ratio (β_{ratio}) as the ratio between β_{sne} and β_{sor} (44). If the β_{ratio} is smaller than 0.5, beta diversity is dominated by turnover rather than nestedness (44).

To disentangle the contribution of stochastic and deterministic community assembly mechanisms while at the same time accounting for possible differences in richness between Z50 and Z400, a null model approach was used. Firstly, the standardized effect size (SES) for pairwise Sørensen ($SES_{\beta sor}$) dissimilarities were estimated in vegan using the oecosimu function. 999 null communities for estimation of $SES_{\beta sor}$ were generated using the quasiswap algorithm (70), which preserve species richness and species incidence. For within groups null model analyses of Z50 and Z400 communities, only the taxa present in Z50 or Z400 respectively were used as the regional species pool. $|SES_{\beta sor}| > 2$ was used as criteria to estimate if $_{\beta sor}$ was different than expected by chance; a $|SES| > 2$ value is approximately a 95% confidence interval (71). Secondly, the RC_{bray} metric (72), which is based on quantitative data, was estimated for between-group comparisons, using 999 simulated communities. $|RC_{bray}| > 0.95$ values were interpreted as deviations from the random expectation (47, 72).

ACKNOWLEDGEMENTS

We thank Fred Sörensson for valuable discussions. The authors acknowledge the Genomics core facility at the University of Gothenburg, the Centre for Cellular Imaging at the University of Gothenburg and the National Microscopy Infrastructure, NMI (VR-RFI 2016-00968), for providing support and use of their equipment, and the colleagues at Veolia Water Technologies AB – AnoxKaldnes, Lund, Sweden, for monitoring the pilot reactor. This work was funded by FORMAS (Contract no. 243-2010-2259, 211-2010-140, 2015-1515-30425-28, 245-2014-1528, 942-2015-683 and 2012-1433), SVU (Contract no. 10-105), the Foundations of Carl Trygger (CTS 12:374), Adlerbertska forskningsstiftelsen, Wilhelm & Martina Lundgrens Vetenskapsfond

(2015-0317, 2015-0309) and the Swedish Water & Wastewater Association via the research cluster VA-teknik Södra.

Conflict of interest: The authors declare no conflict of interest, MP work at Veolia Water Technologies AB – AnoxKaldnes, Lund, Sweden.

REFERENCES

1. Flemming H-C, Wingender J, Szewzyk U, Steinberg P, Rice SA, Kjelleberg S. 2016. Biofilms: An emergent form of bacterial life. Nat Rev Microbiol 14:563-575.
2. Battin TJ, Besemer K, Bengtsson MM, Romani AM, Packmann AI. 2016. The ecology and biogeochemistry of stream biofilms. Nat Rev Microbiol 14:251-263.
3. Costerton JW, Lewandowski Z, Caldwell DE, Korber DR, Lappin-Scott HM. 1995. Microbial biofilms. Annu Rev Microbiol 49:711-745.
4. Leibold MA, Holyoak M, Mouquet N, Amarasekare P, Chase JM, Hoopes MF, Holt RD, Shurin JB, Law R, Tilman D, Loreau M, Gonzalez A. 2004. The metacommunity concept: a framework for multi-scale community ecology. Ecology Lett 7:601-613.
5. Nemergut DR, Schmidt SK, Fukami T, O'Neill SP, Bilinski TM, Stanish LF, Knelman JE, Darcy JL, Lynch RC, Wickey P, Ferrenberg S. 2013. Patterns and processes of microbial community assembly. Microbiol Mol Biol Rev 77:342-356.
6. Zhou J, Ning D. 2017. Stochastic community assembly: Does it matter in microbial ecology? Microbiol Mol Biol Rev 81:e00002-17-32.
7. Battin TJ, Sloan WT, Kjelleberg S, Daims H, Head IM, Curtis TP, Eberl L. 2007. Microbial landscapes: new paths to biofilm research. Nat Rev Microbiol 5:76-81.
8. Vellend M. 2010. Conceptual synthesis in community ecology. Quart Rev Biol 85:183-206.
9. Hubbell SP. 2001. The Unified Neutral Theory of Biodiversity and Biogeography. Princeton University Press, Princeton.
10. Östman Ö, Drakare S, Kritzberg ES, Langenheder S, Logue JB, Lindström ES. 2010. Regional invariance among microbial communities. Ecology letters 13:118-127.
11. Besemer K, Peter H, Logue JB, Langenheder S, Lindström ES, Tranvik LJ, Battin TJ. 2012. Unraveling assembly of stream biofilm communities. ISME J 6:1459-1468.
12. Besemer K, Singer G, Hödl I, Battin TJ. 2009. Bacterial community composition of stream biofilms in spatially variable-flow environments. Appl Environ Microbiol 75:7189-7195.
13. Lyautey E, Jackson CR, Cayrou J, Rols J-L, Garabétian F. 2005. Bacterial community succession in natural river biofilm assemblages. Microb Ecol 50:589-601.

14. Jackson CR, Churchill PF, Roden EE. 2001. Successional changes in bacterial assemblage structure during epilithic biofilm development. Ecology 82:555-566.
15. Langenheder S, Wang J, Karjalainen SM, Laamanen TM, Tolonen KT, Vilmi A, Heino J. 2017. Bacterial metacommunity organization in a highly connected aquatic system. FEMS Microbiol Ecol 93:fiw225.
16. Zhou J, Liu W, Deng Y, Jiang YH, Xue K, He Z, Van Nostrand JD, Wu L, Yang Y, Wang A. 2013. Stochastic Assembly Leads to Alternative Communities with Distinct Functions in a Bioreactor Microbial Community. mBio 4:e00584-12-e00584-12.
17. Ofiţeru ID, Lunn M, Curtis TP. 2010. Combined niche and neutral effects in a microbial wastewater treatment community. Proc Natl Acad Sci USA 107:15345–15350.
18. Ayarza JM, Erijman L. 2010. Balance of neutral and deterministic components in the dynamics of activated sludge floc assembly. Microb Ecol 61:486-495.
19. Griffin JS, Wells GF. 2017. Regional synchrony in full-scale activated sludge bioreactors due to deterministic microbial community assembly. ISME J doi:doi:10.1038/ismej.2016.121:1-12.
20. Lee S-H, Kang H-J, Park H-D. 2015. Influence of influent wastewater communities on temporal variation of activated sludge communities. Water Research 73:132-144.
21. Schramm A, Larsen LH, Revsbech NP, Ramsing NB, Amann R, Schleifer K-H. 1996. Structure and function of a nitrifying biofilm as determined by in situ hybridization and the use of microelectrodes. Appl Environ Microbiol 62:4641-4647.
22. Okabe S, Naitoh H, Satoh H, Watanabe Y. 2002. Structure and function of nitrifying biofilms as determined by molecular techniques and the use of microelectrodes. Water Science and Technology 46:233-241.
23. Almstrand R, Persson F, Hermansson M. 2014. Biofilms in nitrogen removal: Population dynamics and spatial distribution of nitrifying and anammox bacteria. *In* Marco D (ed), Metagenomics of the microbial nitrogen cycle: Theory, methods and applications. Caister Academic Press, Portland, USA
24. Lydmark P, Lind M, Sörensson F, Hermansson M. 2006. Vertical distribution of nitrifying populations in bacterial biofilms from a full-scale nitrifying trickling filter. Environ Microbiol 8:2036-2049.
25. Okabe S, Hiratia K, Ozawa Y, Watanabe Y. 1996. Spatial microbial distributions of nitrifiers and heterotrophs in mixed-population biofilms. Biotechnol Bioeng 50:24-35.
26. Persson F, Wik T, Sörensson F, Hermansson M. 2002. Distribution and activity of ammonia oxidizing bacteria in a large full-scale trickling filter. Water Res 36:1439-1448.
27. Persson F, Sultana R, Suarez M, Hermansson M, Plaza E, Wilén B-M. 2014. Structure and composition of biofilm communities in a moving bed biofilm reactor for nitritation-anammox at low temperatures. Bioresour Technol 154:267-273.
28. Suarez C, Persson F, Hermansson M. 2015. Predation of nitritation–anammox biofilms used for nitrogen removal from wastewater. FEMS Microbiol Ecol 91:fiv124.
29. Ramsing NB, Kuhl M, Jørgensen BB. 1993. Distribution of sulfate-reducing bacteria, O_2, and H_2S in photosynthetic biofilms determined by oligonucleotide probes and microelectrodes. Appl Environ Microbiol 59:3840-3849.
30. Chen J, Hanke A, Tegetmeyer HE, Kattelmann I, Sharma R, Hamann E, Hargesheimer T, Kraft B, Lenk S, Geelhoed JS, Hettich RL, Strous M. 2017. Impacts of chemical gradients on microbial community structure. ISMEJ:1-12.

31. Hall-Stoodley L, Costerton JW, Stoodley P. 2004. Bacterial biofilms: from the Natural environment to infectious diseases. Nat Rev Microbiol 2:95-108.
32. Battin TJ, Kaplan LA, Newbold JD, Cheng X, Hansen C. 2003. Effects of current velocity on the nascent architecture of stream microbial biofilms. Appl Environ Microbiol 69:5443-5452.
33. Hödl I, Mari L, Bertuzzo E, Suweis S, Besemer K, Rinaldo A, Battin TJ. 2013. Biophysical controls on cluster dynamics and architectural differentiation of microbial biofilms in contrasting flow environments. Environ Microbiol 16:802-812.
34. Liu T, Quan X, Li D. 2017. Evaluations of biofilm thickness and dissolved oxygen on single stage anammox process in an up-flow biological aerated filter. Biochem Eng J 119:20-26.
35. He J, Hu H, Qiu W, Liu J, Liu M, Zhao C, Shi X, Xu J. 2016. Community diversity and biofilm characteristic response to low temperature and low C/N ratio in a suspended carrier biofilm reactor. Desal Wat Treat 57:22212–22222.
36. Piculell M, Christensson M, Jönsson K, Welander T. 2016. Partial nitrification in MBBRs for mainstream deammonification with thin biofilms and alternating feed supply. Water Sci Technol 73:1253-1260.
37. Piculell M, Suarez C, Li C, Christensson M, Persson F, Wagner M, Hermansson M, Jönsson K, Welander T. 2016. The inhibitory effects of reject water on nitrifying populations grown at different biofilm thickness. Water Res 104:292-302.
38. Piculell M, Welander P, Jönsson K, Welander T. 2016. Evaluating the effect of biofilm thickness on nitrification in moving bed biofilm reactors. Environ Technol 37:732-743.
39. Torresi E, Fowler SJ, Polesel F, Bester K, Andersen HR, Smets BF, Plósz BG, Christensson M. 2016. Biofilm thickness influences biodiversity in nitrifying mbbrs—implications on micropollutant removal. Environ Sci Technol 50:9279-9288.
40. García S, Trueba A, Vega LM, Madariaga E. 2016. Impact of the surface roughness of AISI 316L stainless steel on biofilm adhesion in a seawater- cooled tubular heat exchanger-condenser. Biofouling 32:1-9.
41. Rao TS. 2009. Comparative effect of temperature on biofilm formation in natural and modified marine environment. Aquat Ecol 44:463-478.
42. Baselga A. 2010. Partitioning the turnover and nestedness components of beta diversity. Global Ecology and Biogeography 19:134-143.
43. Ulrich W, Almeida‐Neto M, Gotelli Nicholas J. 2008. A consumer's guide to nestedness analysis. Oikos 118:3-17.
44. Dobrovolski R, Melo Adriano S, Cassemiro Fernanda AS, Diniz‐Filho José Alexandre F. 2011. Climatic history and dispersal ability explain the relative importance of turnover and nestedness components of beta diversity. Global Ecology and Biogeography 21:191-197.
45. Pjevac P, Schauberger C, Poghosyan L, Herbold CW, van Kessel MAHJ, Daebeler A, Steinberger M, Jetten MSM, Lücker S, Wagner M, Daims H. 2017. AmoA-Targeted Polymerase Chain Reaction Primers for the Specific Detection and Quantification of Comammox Nitrospira in the Environment. Front Microbio 8:847-11.
46. Bell T, Newman Ja, Silverman BW, Turner SL, Lilley AK. 2005. The contribution of species richness and composition to bacterial services. Nature 436:1157-1160.

570 47. Chase JM, Kraft NJB, Smith KG, Vellend M, Inouye BD. 2011. Using null models to
571 disentangle variation in community dissimilarity from variation in α-diversity. Ecosphere
572 2:art24-11.
573 48. Pagaling E, Vassileva K, Mills Catherine G, Bush T, Blythe Richard A, Schwarz-Linek J,
574 Strathdee F, Allen Rosalind J, Free A. 2017. Assembly of microbial communities in
575 replicate nutrient-cycling model ecosystems follows divergent trajectories, leading to
576 alternate stable states. Environmental Microbiology 19:3374-3386.
577 49. Strous M, Van Gerven E, Kuenen J, Jetten M. 1997. Effects of aerobic and microaerobic
578 conditions on anaerobic ammonium-oxidizing (anammox) sludge. Appl Environ Microbiol
579 63:2446–2448.
580 50. Chen H, Athar R, Zheng G, Williams HN. 2011. Prey bacteria shape the community
581 structure of their predators. ISME J 5:1314-1322.
582 51. Chen H, Young S, Berhane T-K, Williams HN. 2012. Predatory *Bacteriovorax*
583 communities ordered by various prey species. PLoS ONE 7:e34174-11.
584 52. Torsvik V, Ovreas L, Thingstad TF. 2002. Prokaryotic diversity - Magnitude, dynamics,
585 and controlling factors. Science 296:1064-1066.
586 53. Feng S, Tan CH, Cohen Y, Rice SA. 2016. Isolation of *Bdellovibrio bacteriovorus* from a
587 tropical wastewater treatment plant and predation of mixed species biofilms assembled by
588 the native community members. Environ Microbiol 18:3923-3931.
589 54. Wittebolle L, Marzorati M, Clement L, Balloi A, Daffonchio D, Heylen K, De Vos P,
590 Verstraete W, Boon N. 2009. Initial community evenness favours functionality under
591 selective stress. Nature 458:623-626.
592 55. Peter H, Beier S, Bertilsson S, Lindström ES, Langenheder S, Tranvik LJ. 2010. Function-
593 specific response to depletion of microbial diversity. ISME J 5:351-361.
594 56. Knelman JE, Nemergut DR. 2014. Changes in community assembly may shift the
595 relationship between biodiversity and ecosystem function. Front Microbiol 5:Article 424,
596 1-4.
597 57. Hillebrand H, Bennett D, M, Cadotte M, W. 2008. Consequences of dominance: A review
598 of evenness effects on local and regional ecosystem processes. Ecology 89:1510-1520.
599 58. Okabe S, Satoh H, Watanabe Y. 1999. In situ analysis of nitrifying biofilms as determined
600 by in situ hybridization and the use of microelectrodes. Appl Environ Microbiol 65:3182-
601 3191.
602 59. Schmidt I, van Spanning RJM, Jetten MSM. 2004. Denitrification and ammonia oxidation
603 by Nitrosomonas europaea wild-type, and NirK- and NorB-deficient mutants.
604 Microbiology 150:4107-4114.
605 60. Mori AS, Isbell F, Seidl R. 2018. β-Diversity, Community Assembly, and Ecosystem
606 Functioning. Trends in Ecology & Evolution 33:549-564.
607 61. Persson F, Suarez M, Hermansson M, Plaza E, Wilén B-M. 2016. Community structure of
608 partial nitritation-anammox biofilms at decreasing substrate concentrations and low
609 temperature Microb Biotechnol 154:267-273.
610 62. Callahan BJ, McMurdie PJ, Holmes SP. 2017. Exact sequence variants should replace
611 operational taxonomic units in marker-gene data analysis. ISME J 11:2639-2643.
612 63. Edgar RC. 2016. UNOISE2: improved error-correction for Illumina 16S and ITS amplicon
613 sequencing. bioRxiv doi:doi: http://dx.doi.org/10.1101/081257:1-21.
614 64. McMurdie PJ, Holmes S. 2013. phyloseq: An R Package for Reproducible Interactive
615 Analysis and Graphics of Microbiome Census Data. PLOS ONE 8:e61217.

65. Oksanen J, Blanchet FG, Friendly M, Kindt R, Legendre P, McGlinn D, Minchin PR, O'Hara RB, Simpson GL, Solymos P, Stevens MHH, Szoecs E, Wagner H. 2017. vegan: Community Ecology Package, https://CRAN.R-project.org/package=vegan.
66. Love MI, Huber W, Anders S. 2014. Moderated estimation of fold change and dispersion for RNA-seq data with DESeq2. Genome Biol 15:550.
67. McMurdie PJ, Holmes S. 2014. Waste Not, Want Not: Why Rarefying Microbiome Data Is Inadmissible. PLOS Computational Biology 10:e1003531.
68. Jost L. 2006. Entropy and diversity. Oikos 113:363-375.
69. Anderson MJ. 2001. A new method for non-parametric multivariate analysis of variance. Austral Ecology 26:32-46.
70. Miklós I, Podani J. 2004. Randomization of presence - absence matrices: comments and new algorithms. Ecology 85:86-92.
71. Gotelli NJ, McCabe DJ. 2002. Species co-occurrence: a meta-analysis of j. M. Diamond's assembly rules model. Ecology 83:2091-2096.
72. Stegen JC, Lin X, Fredrickson JK, Chen X, Kennedy DW, Murray CJ, Rockhold ML, Konopka A. 2013. Quantifying community assembly processes and identifying features that impose them. ISME J 7:2069-2079.

FIGURE LEGENDS

Fig 1. Biofilm structure shown by EPS staining of cryosections. The biofilm-water interface is the upper side. A. Z400 biofilm. B: Z50 biofilm. Scale bar: 100 µm. (C): Z400 (up) and Z50 (down) biofilm carriers; a ruler in cm is shown for size comparison.

Fig 2. A: Richness (^0D), diversity (^1D) and evenness ($^1D/\,^0D$) for the Z50 and Z400 biofilms. B: PCoA based on the Sørensen index (β_{sor}).

Fig 3. (A) Standardized effect size for the Sørensen index (β_{sor}); dashed lines indicate SES values of +2 and -2. B: β_{sne} (dissimilarity due to nestedness) and β_{sim} (turnover) values; the sum of β_{sim} and β_{sne} is β_{sor}. (C) Beta diversity ratio. Values were estimated for pairwise comparisons among Z400 replicates (n=10), Z50 replicates (n=10) and between the two groups.

644 **Fig. 4.** (A) Relative read abundance of nitrifiers and anammox bacteria in Z50 and Z400. (B)
645 Relative read abundance multiplied by total solids (TS) measurements for each carrier type. (C)
646 Biovolume fractions of nitrifiers and anammox bacteria, as measured by qFISH.

647 **Fig. 5.** (A) FISH image of a Z400 biofilm cryosection; the water-biofilm interface is on the top.
648 Green: *Nitrosomonas*. Red: *Nitrospira*. Yellow: *Nitrotoga*. Blue: *Brocadia*. Grey: SYTO. (B)
649 FISH-based population distribution at different biofilm depths in Z400. (C) FISH image of a Z50
650 biofilm cryosection; the water-biofilm interface is on the top. Green: *Nitrosomonas*. Red:
651 *Nitrospira*. Yellow: *Nitrotoga*. Grey: SYTO.

652 **Fig. 6.** DO concentrations profiles in the Z50 and Z400 biofilms. The shaded regions show
653 ranges of DO concentration profiles resulting from different assumption about the fraction of the
654 total dry solids on the carriers that is active bacteria. The dashed horizontal lines show the
655 biofilm-liquid interface.

656 **Fig. 7.** Potential conversion rates by carrier type during aerobic oxidation of NH4+ (A), aerobic
657 oxidation of NO2- (B) and anoxic oxidation of NH4 (C) during batch tests. Significant
658 differences between Z50 and Z400 (ANCOVA, $p<0.05$) are shown with (*) . Red: Z400, Blue:
659 Z50.

660

661

662 **SUPPLEMENTAL INFORMATION**

663 **Fig. S1. Log2fold (DESeq2) changes for the 40 most abundant SVs based on average**
664 **abundance**

665 Phylum, order and genus classification are shown. Each circle represents an SV. The size of the
666 circle is proportional to the total sequence read abundance for the SV. A negative log2 fold
667 change indicates that SV are more abundant in Z400 biofilm, while a positive log2 fold change
668 indicates SVs more abundant in Z50 biofilms.

669 **Fig. S2. Log2fold (DESeq2) changes for *Bdellovibrionales* SVs.**

670 Genus classification is shown. Each circle represents an SV. The size of the circle is proportional
671 to the total sequence read abundance for the SV. A negative log2 fold change indicates that SV
672 are more abundant in Z400 biofilm, while a positive log2 fold change indicates SVs more
673 abundant in Z50 biofilms. SVs with a NA $p_{(adj)}$ value (DESeq2) are not shown.

674 **Fig. S3. Density profiles and biomass distribution for the DO model**

675 A and B: Biofilm density profiles (total dry solids) in the Z50 and Z400 biofilms respectively. C:
676 Assumed biomass distribution in the Z400 biofilm based on input from qFISH and cryosection
677 FISH images

678 **Table S1.** FISH probes used in this study

679 **Table S2**. Notation used in the DO model.

680 **Table S3.** Kinetic rate expressions used in the DO model.

681 **Table S4.** Stoichiometric matrix used in the DO model

682 **Table S5**. Kinetic and stoichiometric coefficients used in the DO model.

683 **Table S6**. Default input values for physical parameters used in the DO model.

684 **Text S1.** Supplemental Material and Methods

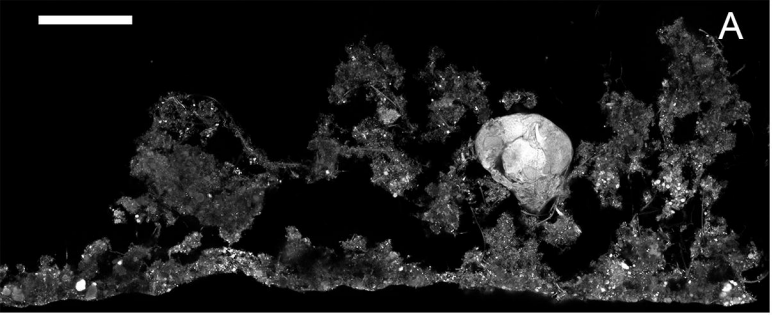
A
B
C
0
1
2
3
4
5
6
7

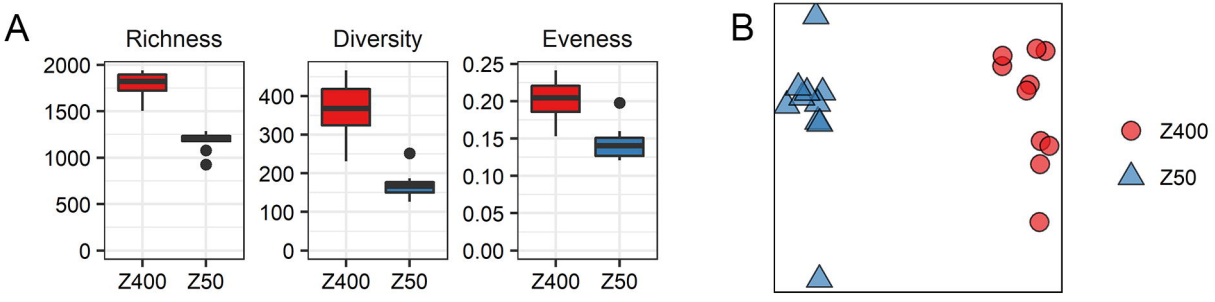
A
Richness
Diversity
Eveness
2000
1500
1000
500
0
400
300
200
100
0
0.25
0.20
0.15
0.10
0.05
0.00
Z400
Z50
Z400
Z50
Z400
Z50
B
Z400
Z50

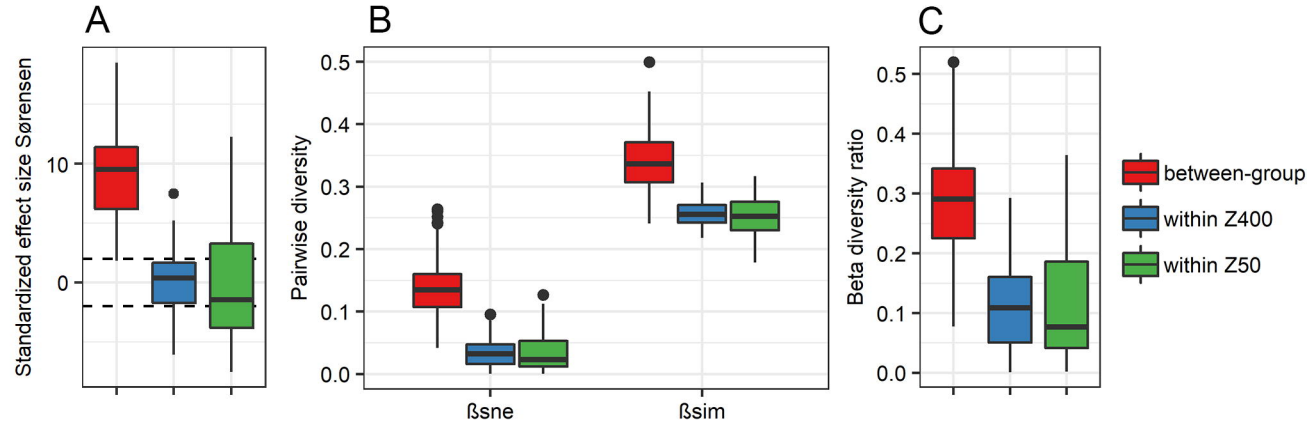
A
B
C
Standardized effect size Sørensen
10
0
Pairwise diversity
0.5
0.4
0.3
0.2
0.1
0.0
ßsne
ßsim
Beta diversity ratio
0.5
0.4
0.3
0.2
0.1
0.0
between-group
within Z400
within Z50

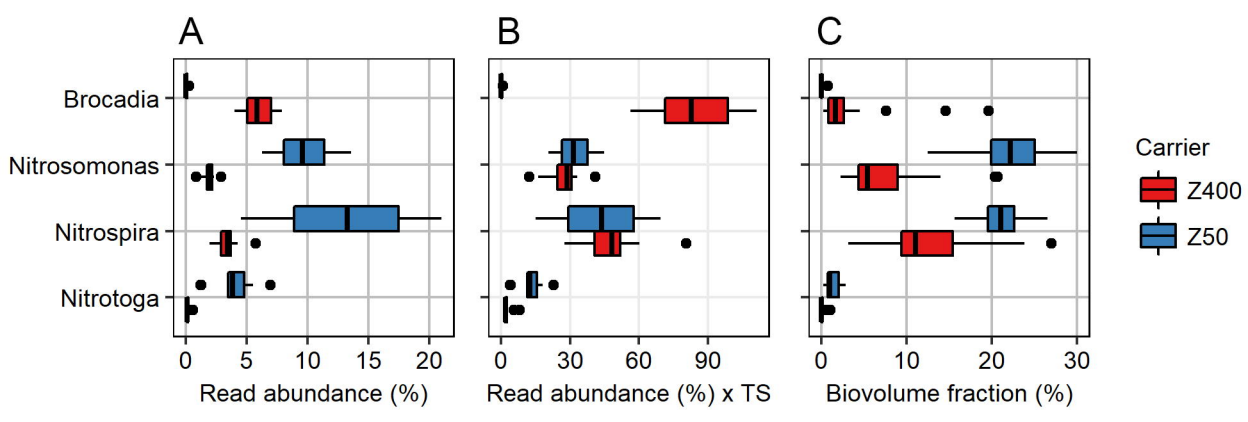
A
B
C
Brocadia
Nitrosomonas
Nitrospira
Nitrotoga
0
5
10
15
20
Read abundance (%)
0
30
60
90
Read abundance (%) x TS
0
10
20
30
Biovolume fraction (%)
Carrier
Z400
Z50

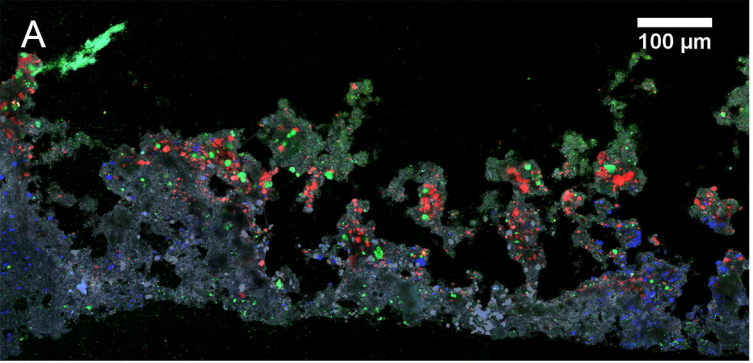
A
100 µm

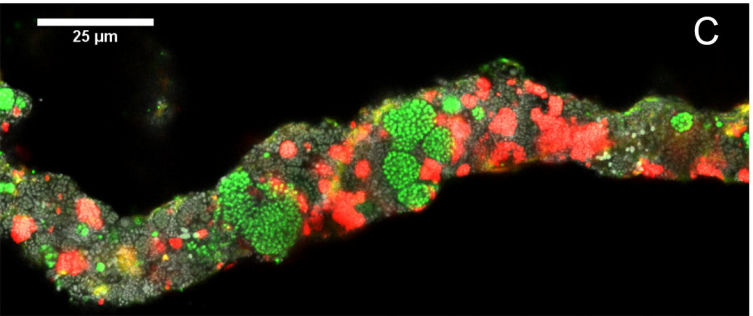
25 µm
C

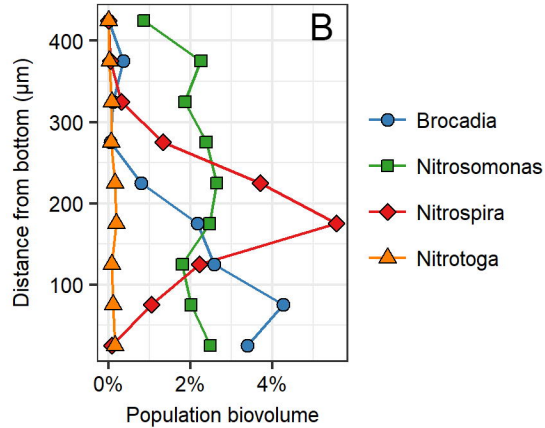
B
Distance from bottom (µm)
400
300
200
100
0%
2%
4%
Population biovolume
Brocadia
Nitrosomonas
Nitrospira
Nitrotoga

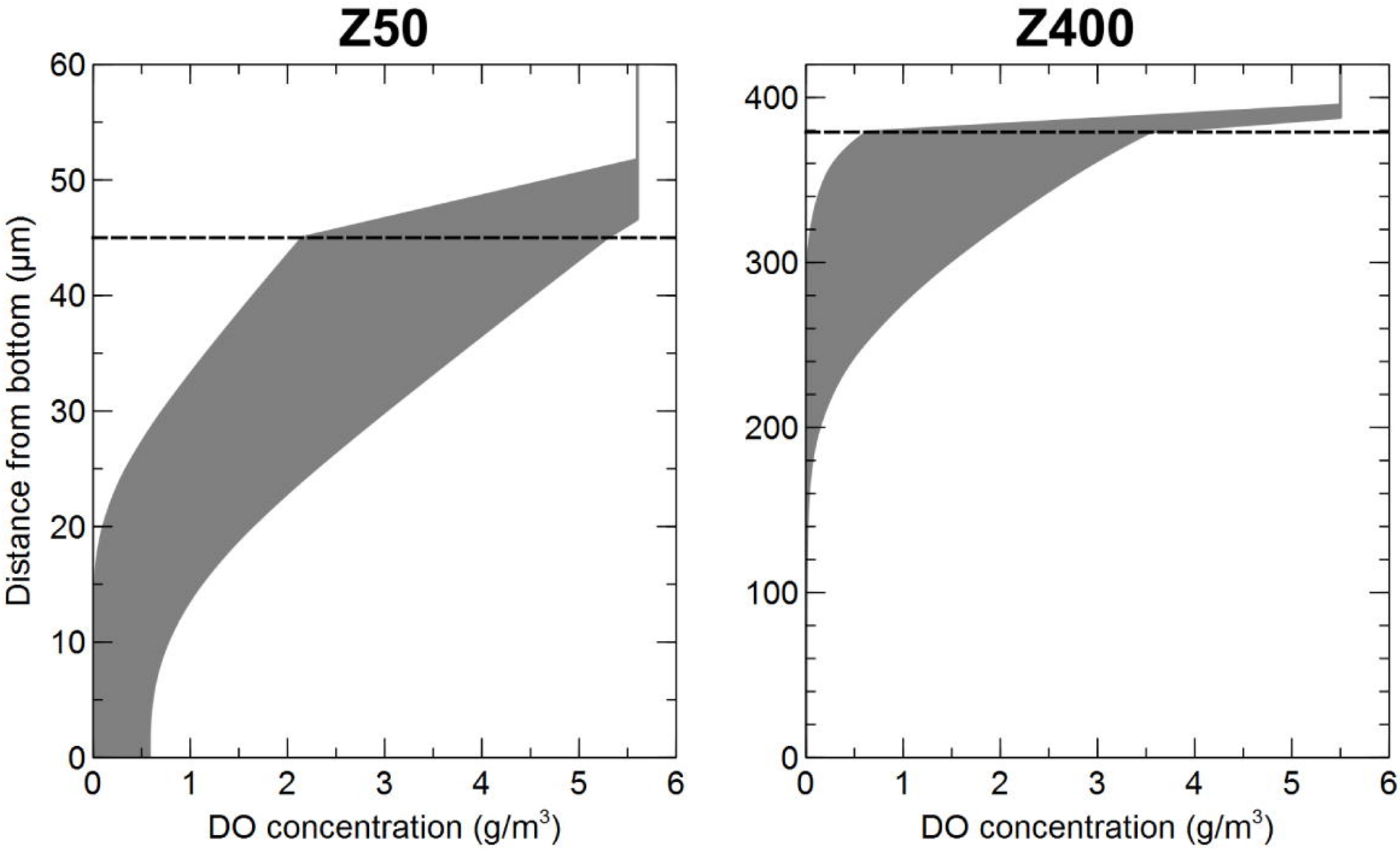
Z50
Z400
Distance from bottom (μm)
DO concentration (g/m3)
DO concentration (g/m3)
0
10
20
30
40
50
60
100
200
300
400
0
1
2
3
4
5
6

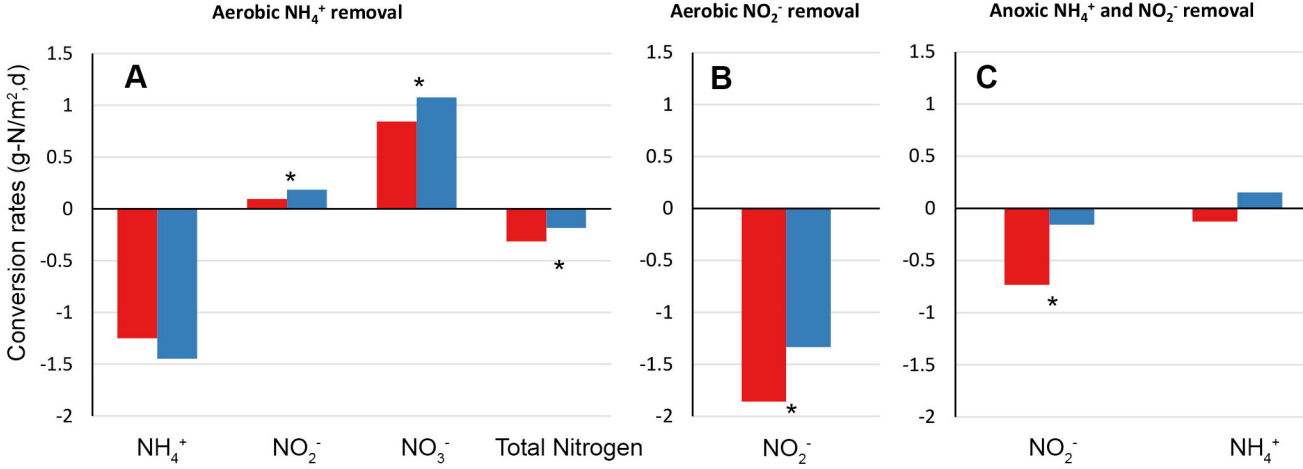
Aerobic NH_4^+ removal
Aerobic NO_2^- removal
Anoxic NH_4^+ and NO_2^- removal
A
B
C
Conversion rates (g-N/m^2,d)
1.5
1
0.5
0
-0.5
-1
-1.5
-2
*
NH_4^+
NO_2^-
NO_3^-
Total Nitrogen
NO_2^-
NO_2^-
NH_4^+